









## RESEARCH ARTICLE

# Tree species explain only half of explained spatial variability in plant water sensitivity

Alexandra G. Konings<sup>1</sup>  | Krishna Rao<sup>1,2</sup>  | Erica L. McCormick<sup>1</sup>  |  
 Anna T. Trugman<sup>3</sup>  | A. Park Williams<sup>4</sup>  | Noah S. Diffenbaugh<sup>1</sup>  | Marta Yebra<sup>5,6</sup>  |  
 Meng Zhao<sup>7</sup> 

<sup>1</sup>Department of Earth System Science, Stanford University, Stanford, California, USA

<sup>2</sup>Watershed, Inc., San Francisco, California, USA

<sup>3</sup>Department of Geography, University of California, Santa Barbara, California, USA

<sup>4</sup>Department of Geography, University of California, Los Angeles, California, USA

<sup>5</sup>Fenner School of Environment & Society, The Australian National University, Canberra, Australian Capital Territory, Australia

<sup>6</sup>School of Engineering, The Australian National University, Canberra, Australian Capital Territory, Australia

<sup>7</sup>Department of Earth and Spatial Science, University of Idaho, Moscow, Idaho, USA

## Correspondence

Alexandra G. Konings, Department of Earth System Science, Stanford University, Stanford, CA, USA.

Email: [konings@stanford.edu](mailto:konings@stanford.edu)

## Funding information

Earth Sciences Division, NASA, Grant/Award Number: 80NSSC21K1523; National Science Foundation, Grant/Award Number: 1942133, 2003205 and 2216855; Gordon and Betty Moore Foundation, Grant/Award Number: 11974

## Abstract

Spatiotemporal patterns of plant water uptake, loss, and storage exert a first-order control on photosynthesis and evapotranspiration. Many studies of plant responses to water stress have focused on differences between species because of their different stomatal closure, xylem conductance, and root traits. However, several other ecohydrological factors are also relevant, including soil hydraulics, topographically driven redistribution of water, plant adaptation to local climatic variations, and changes in vegetation density. Here, we seek to understand the relative importance of the dominant species for regional-scale variations in woody plant responses to water stress. We map plant water sensitivity (PWS) based on the response of remotely sensed live fuel moisture content to variations in hydro-meteorology using an auto-regressive model. Live fuel moisture content dynamics are informative of PWS because they directly reflect vegetation water content and therefore patterns of plant water uptake and evapotranspiration. The PWS is studied using 21,455 wooded locations containing U.S. Forest Service Forest Inventory and Analysis plots across the western United States, where species cover is known and where a single species is locally dominant. Using a species-specific mean PWS value explains 23% of observed PWS variability. By contrast, a random forest driven by mean vegetation density, mean climate, soil properties, and topographic descriptors explains 43% of observed PWS variability. Thus, the dominant species explains only 53% (23% compared to 43%) of explainable variations in PWS. Mean climate and mean NDVI also exert significant influence on PWS. Our results suggest that studies of differences between species should explicitly consider the environments (climate, soil, topography) in which observations for each species are made, and whether those environments are representative of the entire species range.

This is an open access article under the terms of the [Creative Commons Attribution](https://creativecommons.org/licenses/by/4.0/) License, which permits use, distribution and reproduction in any medium, provided the original work is properly cited.

© 2024 The Author(s). *Global Change Biology* published by John Wiley & Sons Ltd.

## KEYWORDS

inter-specific variability, intra-specific variability, live fuel moisture content, plant hydraulic traits, plant-water interactions, water stress

## 1 | INTRODUCTION

The response of plants to water stress has myriad effects on local ecosystems and water cycling. It is a first-order control on evapotranspiration (ET, Pappas et al., 2016) and thus a key determinant of water availability for human consumption (Mastrotheodoros et al., 2020; Seager et al., 2013; Ukkola, Prentice, et al., 2016), land-atmosphere interactions, and drought and heatwave evolution (Miralles et al., 2019). Additionally, plant water stress responses also affect rates of photosynthesis (Pappas et al., 2016), vegetation growth, mortality, and wildfire risk (Brodribb et al., 2020). As a result, they are also a significant control on vegetation's potential to sequester carbon (Anderegg et al., 2020; Coffield et al., 2021; Wu et al., 2023).

Despite significant concerted research effort (Brodribb et al., 2020; Grossiord et al., 2020), the response of vegetation to water stress remains poorly understood. Development of a reliable model of stomatal closure has been argued to be one of the holy grails of plant physiology (Buckley, 2017), but continues to be uncertain and error-prone (Sabot et al., 2022; Wang et al., 2021). Land surface models overestimate the impact of droughts (Ukkola, De Kauwe, et al., 2016) and often cannot even predict the sign of ET's response to drought (Zhao et al., 2022). Compensation and cross-correlation between drought's dual effects of increasing vapor pressure deficit (VPD) and reduced root-zone soil moisture add further complexity (Liu et al., 2020; Novick et al., 2016; Vargas Zeppetello et al., 2023). Efforts to reduce these uncertainties are hindered by the large range of processes across the soil-plant-atmosphere continuum that influence the effect of hydrometeorology on plants. For example, precipitation anomalies may translate non-linearly to anomalies in root-zone water availability due to soil-dependent variations in infiltration rates, water storage, and topography-induced lateral redistribution of water (e.g., Hahm et al., 2019; Miguez-Macho & Fan, 2021; Paschalis et al., 2022). The resulting anomalies in the three-dimensional distribution of root-zone soil water content are then mediated by a large range of plant traits—including those affecting plant rooting depth and distribution, root conductance and root water uptake, rates of water movement through the plant xylem, and stomatal closure (Fatichi et al., 2016). Here, we collectively refer to these traits as 'plant hydraulic traits'.

Because plant hydraulic traits vary significantly by species (Bartlett et al., 2016; Skelton et al., 2015), many studies of plant drought and water stress response analyze vegetation behavior as a function of species (e.g., Brzostek et al., 2014; Cabon et al., 2023; Serra-Maluquer et al., 2022). However, the focus on species-by-species differences in studies of plant water stress neglects the fact that plant hydraulic traits may exhibit significant intra-specific variability (González de Andrés et al., 2021; Kannenberg et al., 2022; Lu

et al., 2022), including through adaptation to local climate (Depardieu et al., 2020; Pritzkow et al., 2020). It also ignores the potential role of soil and topography variations and their interactions with species-specific physiologies.

To make progress on understanding the response of plants to water stress, it is therefore necessary to understand the relative contributions of species, soil, topography, and climate to the overall response of vegetation to water stress. To this end, several studies have analyzed the sources of spatial variability for various water stress response indices (e.g., Felton et al., 2021; Fu et al., 2022; Ukkola et al., 2021; Yang et al., 2022). However, these studies have focused on analyzing metrics that are not solely related to water stress. For example, Green et al. (2022) analyzed the ratio of land surface temperature to air temperature (an indirect proxy for sensible heat), which is also influenced by variations in other meteorological drivers (i.e., radiation, surface roughness, wind speed) even in the absence of changes in water stress. Other studies have focused on spatial variability of the response of net primary productivity (NPP) to precipitation (Felton et al., 2021; Ukkola et al., 2021). However, NPP combines plant responses to water stress along multiple axes, including photosynthesis, respiration, and water uptake. Furthermore, in order to study a large spatial extent, and because species information is rarely available over large areas (and thus, rarely considered in large-scale studies), few studies have considered the role of species (though see D'Orangeville et al. (2018) and Gazol et al. (2017) for exceptions).

In this study, we quantify "plant water sensitivity" (PWS) by comparing the dynamics of live fuel moisture content (LFMC) (which quantifies the relative water content of plant canopies) with dead fuel moisture content (a proxy for how LFMC would be expected to evolve in response to hydrometeorology in the absence of soil, plant water uptake, and transpiration processes). We take advantage of a recently derived high-resolution map of plant water sensitivity across the western United States (Rao et al., 2022), a region that covers a variety of climatic and biogeographic conditions. We then analyze the degree to which species, plant traits, climate, soil type, and topography control the spatial variability in LFMC sensitivity to climate at a large number of locations where a single species is dominant and identified.

## 2 | METHODS

## 2.1 | Plant water sensitivity mapping

We create and analyze maps of PWS, which quantify the integrated sensitivity of vegetation water to hydroclimate. To estimate PWS, we follow an approach previously used in Rao et al. (2022). The approach is based on the recognition that moisture content in both soil and plants has memory (McColl et al., 2017), and that plant water sensitivity must therefore take into account both current and past meteorology. The first step in the calculation of the PWS is to perform a multiple linear regression between the LFMC (defined as the

weight of water stored in vegetation divided by the dry vegetation weight) and dead fuel moisture content (DFMC, a metric of climate). Specifically, this regression is calculated as:

$$\text{LFMC}_t = \sum_{i=0}^{N=8} \beta_i \times \text{DFMC}_{t-i} + \gamma \quad (1)$$

Above, the index  $t$  represents the time steps of the data, and  $i$  is an index describing the number of lagged 15-day timesteps. A 15-day timestep is used because it is the timestep of the remotely sensed LFMC dataset, which is described below. The  $N$  corresponds to the number of lagged timesteps used in the regression. We then calculate a static map of PWS as the sum of the slopes  $\beta_i$  of the multiple linear regression:

$$\text{PWS} = \sum_{i=1}^{N=8} \beta_i \quad (2)$$

In the above equations, the  $i$  denotes 15-day timesteps across which average LFMC and DFMC are used and  $\gamma$  is the intercept of the regression. The optimal timescale likely varies from location to location and from season to season (e.g., it may be wetter during seasons with more frequent rain than during a dry, Mediterranean-type summer) (Knighton & Berghuijs, 2023; Liu et al., 2018). Here, we use  $N=8$ , representing a memory timescale of about 4 months, since it represents a reasonable average of previously calculated water memory timescales in vegetation across the western United States (Liu et al., 2018).

We use 100-h DFMC as the independent metric of hydroclimate in Equation (1) because it represents the integrated influence of atmospheric conditions (i.e., precipitation and atmospheric water demand) on vegetation in the absence of modifications due to soil infiltration or vegetation (Matthews, 2014). Specifically, the DFMC is calculated considering both the effect of precipitation in the previous 24 h and the drying power of the atmosphere (dependent on temperature and relative humidity) to determine the equilibrium moisture content of the dead fuels (Cohen & Deeming, 1985). The calculation is adjusted based on the duration of daylight at a given latitude (Cohen & Deeming, 1985). The DFMC can be calculated for different fuel classes. Here, the 100-h DFMC is chosen because it represents the wetness of twigs and branches of a few centimeters in diameter (Burgan, 1988), which is similar to the vegetation elements contributing the most to the remotely sensed LFMC (Rao et al., 2022).

The DFMC has the same units (amount of water per amount of dry biomass) as LFMC, facilitating interpretation of the slope magnitudes  $\beta_i$ , which are unitless. To keep the influence of  $\text{DFMC}_t$  on LFMC physically plausible, the regression in Equation (1) is constrained to only use non-negative values of  $\beta_i$ . Overall, low values of  $\beta_i$  suggest that LFMC does not decrease as quickly when DFMC decreases, because of soil or plant mechanisms that limit the effect of the climate-induced DFMC reductions. Thus, ecosystems with lower PWS are less sensitive to water stress.

We use a time series of LFMC derived from Sentinel-1 SAR observations (which are sensitive to canopy water content across much of the canopy depth) and Landsat canopy reflectances. It is based on a machine learning approach trained on in situ observations of LFMC from the National Fuel Moisture Database (Rao et al., 2020). The record spans the western United States; the eastern boundary of this region consists of and includes the states of Montana, Wyoming, Colorado, and Texas. It has a 250 m spatial resolution and a 15-day temporal resolution. More details of the LFMC dataset can be found in Rao et al. (2020). The 100-h DFMC record is based on GRIDMET (Abatzoglou, 2013). PWS is calculated across the period from 2016 to 2021, coinciding with Sentinel-1A and Sentinel-1B availability. Note that unlike the PWS maps used in Rao et al. (2022), which were calculated only based on the summer fire season, here we calculate PWS across the entire year. As part of the calculation, LFMC is re-sampled to match the 4 km resolution of DFMC, and DFMC data are linearly averaged to match the 15-day temporal resolution of LFMC, generating a static spatial map of PWS at 4 km.

## 2.2 | Calculating species influence on PWS

Our analysis is focused on locations with field plots in the US Forest Service Forest Inventory and Analysis (FIA) program (Bechtold et al., 2005; Gray et al., 2012), the United States' program of intensively sampled long-term inventory plots. As such, we focus only on forested locations. Focusing on only these plot locations provides information about species composition in each location, since continuous maps of species composition are not available across the entire western United States. Furthermore, we focus only on FIA plots where at least 75% of the basal area is from a single species. We interpret these locations as ones where a single species dominates the biomass and thus, the PWS. Limiting our focus to such pixels allows for analysis of the impact of species on PWS, which would be impossible at mixed-species sites because there is not enough information to deduce how much of the PWS at a given site is influenced by each of the different species present there.

Limiting our focus to 'single-species' locations reduces the number of 4 km pixels containing one or more FIA plots from 48,305 to 28,940, or about 60% of the original number. Of these, a small subset is missing one of the soil, plant, and topographic factors used for comparison (see below) and is removed from the analysis. Additionally, we also remove pixels where the dominant land cover is grassland, pasture, or mixed forest (as estimated from the 2016 National Land Cover Database (Fry et al., 2011)), since in these pixels, the FIA plots' dominant species cannot be representative of the entire PWS pixel. After these filters, 21,445 pixels remain in our analysis (Figure 1a). Focusing on plots where only a single species dominates the basal area is likely to bias the distribution of species studied to some degree relative to the full distribution of species composition across the western United States. Therefore, we further analyze the distribution of species remaining in the final plots to ensure that the most common tree species are well represented in the final dataset.

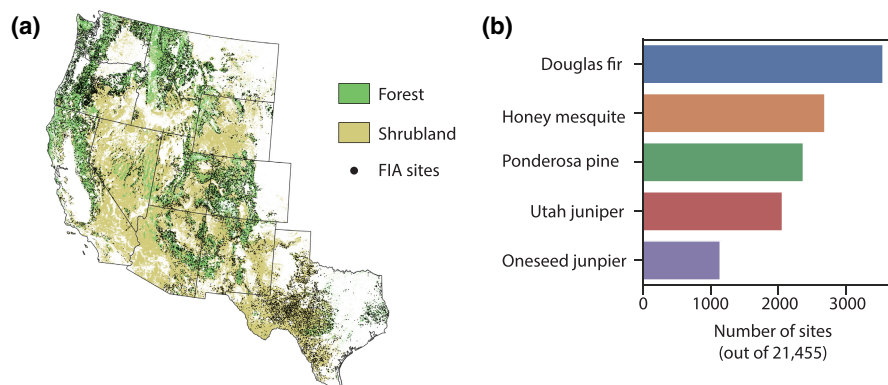


**FIGURE 1** FIA plots considered for this study. Panel (a) shows the map of the FIA plots used in this study, overlaid on a National Land Cover Database 2021 map of forests and shrublands. Panel (b) shows the number of sites for the top five most common species in the dataset.

Having identified the 21,445 pixels where a single species can be assumed dominant, we calculate the influence of the dominant species on PWS as the coefficient of determination ( $R^2$ ) between observed PWS and a model that predicts PWS based on species-specific means alone. Note that we use the phrase 'observed PWS' here for simplicity, but that it is estimated from a regression of observed LPMC, rather than being directly observed. For each pixel, this model predicts PWS as the mean observed PWS of all pixels in which the dominant species is the same as at the pixel under consideration. This is the mathematically optimal PWS prediction model based on species information alone—no other formulation would achieve higher  $R^2$  unless other information was used.

There is some spatial mismatch in our approach. The PWS is calculated at 4 km and thus each pixel contains an area of 16 km<sup>2</sup>. FIA plots are more than a thousand times smaller, with only a subset of a ~4000 m<sup>2</sup> area sampled at each site. Furthermore, the identified location of each FIA plot is fuzzed within a 1.6 km radius to protect landowner privacy and protect the integrity of the plot. Additionally, plot locations on private lands are swapped in up to 20% of cases, although such swaps are contained to the same county and to plots with the same ecotype (Burrill et al., 2021; Gray et al., 2012). Here, we assume that if a single species is dominant in an FIA plot, this dominance is also in effect across the entire 4 km PWS pixel. Upon making this assumption, it follows that in most cases a 1.6 km random offset away from a marked FIA location would not change the PWS pixel in which it falls, and nor would a swap with another same-ecotype plot in the same county. Thus, this location uncertainty does not change the implied match between the PWS pixel and which species is dominant there. Overall, our analysis rests on the assumption that the advantage of being able to study plant water sensitivity across tens of thousands of sites outweighs the errors induced by the presence of some differences in spatial representativeness differences. The impact of the resolution differences on the interpretation of the results is examined in the Discussion (Section 4) below.

### 2.3 | Comparison to other predictive factors

The  $R^2$  between observed PWS and PWS predicted by species-specific means is difficult to interpret in isolation. It is unclear how

much of the  $R^2$  is attributable to the magnitude of the noise in our species dominance and PWS calculations (particularly in light of the resolution difference mentioned above), and how much is due to the true limitations in using the dominant species as the sole predictor of PWS. To provide further context, we compare the  $R^2$  of the species-cover-based predictions to the  $R^2$  of a random forest model that provides an estimate of how much of the spatial variability in PWS can be explained by other factors, including soil, plant, and topographic factors. This random forest model does not include species information. The random forest model contains 120 "trees", and tests up to 10 features per split. These hyperparameters were chosen by testing a range of possible values and selecting those that led to the best model performance. In addition, the random forest model has a maximum tree depth of 8, which balances sufficient depth to improve performance and avoiding over-fitting. The model is tested with 10-fold cross-validation. The importance of different input features to the final random forest model is calculated based on the permutation feature importance—the decrease in model score when a feature is randomly shuffled. We used Python's scikit-learn package version 0.24.2 to fit the random forest model and analyze the feature importance.

We considered a variety of possible features for inclusion in the random forest model, representing local climate characteristics, stand density proxies, soil, and topographic factors. The features considered, whether they were selected for the final model, and their data sources are summarized in Table S1. As possible climate characteristics, we test the mean monthly value and the monthly coefficient of variation of VPD, temperature, and precipitation, as well as the aridity index. The coefficient of variation is used as a measure of how variable the climatic driver is across the year, and is calculated as the standard deviation of the long-term mean of each month, divided by the overall mean monthly value. We use the coefficient of variation rather than the standard deviation, as the latter is highly correlated with the mean for several drivers. These climate data are derived from PRISM (Daly et al., 2008, 2015). The aridity index is calculated as the ratio of mean potential evapotranspiration (PET) to mean precipitation, calculated over the period 1981–2010, with the GridMET-calculated PET based on the Penman-Monteith method (Abatzoglou, 2013). As vegetation density proxies, we use mean NDVI (calculated as the long-term

average across the 2001–2020 record of the MODIS MOD13Q1 V6.1 NDVI product (Didan et al., 2021)), lidar-derived canopy height (from IceSat GLAS (Simard et al., 2011)), and aboveground biomass. The aboveground biomass dataset is based on a machine learning algorithm that combines inventory data, airborne laser scanning, and spaceborne lidar and radar data to estimate aboveground biomass (Xu et al., 2021). The specific soil proxies used are based on the data available from the gridded National Soil Survey Geographic Database (gNATSGO) dataset. We use gNATSGO instead of other soil property datasets since it is based solely on data from detailed field surveys and avoids errors associated with digital soil mapping (Rossiter et al., 2022). In particular, we use four gNATSGO variables: (i) soil bulk density, given that it is inversely related to soil porosity, which would be expected to influence how much water soils can store after saturating rain events; (ii) total available water storage; (iii) saturated hydraulic conductivity, given that it controls the rate of runoff generation and leakage out of the root zone; and (iv) the soil moisture at 1/3rd bar as a measure of soil retention. The gNATSGO data is available across several depth layers, but the optimal depth is likely variable from location to location (e.g., depending on local soil layers and bedrock depth). Considering depths that are too small may induce some error because changes in soil properties that are below the considered depth but still within the rooting zone would not be accounted for. Alternatively, depths that are too large may include information about soil profiles that are not relevant to the rooting zone. Here, we use the 0 to 50 cm average as a reasonable value for most gNATSGO-derived soil properties, but use the 0 to 150 cm values for the available water storage (although note that if bedrock is shallower than 150 cm, gNATSGO automatically calculates available water storage only to the soil depth). Beyond the above properties, we also test an estimate of the total root-zone water storage capacity (abbreviated as RZ storage in the figure legends) derived from McCormick et al. (2021). This dataset is not tied to a particular depth and accounts for water storage in both soil and bedrock, given that bedrock water use is considerably more widespread in the western United States than generally appreciated (McCormick et al., 2021). The root-zone water storage capacity is calculated based on a mass balance approach by determining the

maximum accumulation of evapotranspiration in excess of precipitation over a multi-year period. Finally, as topographic features, we consider the local slope and aspect (obtained from the National Elevation Dataset), as well as two indices intended to capture the effect of topography on hydrology. Specifically, we consider the height-above-nearest drainage (that is, the elevation difference between the local point and the nearest point of drainage, based on calculating drainage directions from a digital elevation model), and the topographic wetness index (i.e., the ratio of the log of the total catchment area per unit flow width and the tangent of the slope, (Beven & Kirkby, 1979)). Both of these datasets are derived from MERIT HYDRO (Yamazaki et al., 2019). All random forest inputs used are originally calculated at the native resolution of the associated dataset, and then interpolated to 4 km to match the resolution of the PWS dataset.

To enable interpretation of the final feature influence, we eliminate features with a cross-correlation  $r > .70$ . For example, because the height-above-nearest-drainage and the slope have a cross-correlation of  $r = .85$ , only slope is included in the final model. In cases of cross-correlation between two features, the feature with the lowest univariate correlation with PWS is removed, and the other feature retained. Other features removed because of high cross-correlations included the mean precipitation, mean temperature, coefficient of variation of VPD, and coefficient of variation of temperature. All vegetation density and size proxies were cross-correlated (e.g.,  $r_{\text{NDVI, canopy height}} = .72$  &  $r_{\text{NDVI, AGB}} = .75$ ,  $r_{\text{canopy height, AGB}} = .72$ ), so this axis is summarized using the single feature of mean NDVI, although we note that the greenness of a given level of biomass or density also affects NDVI to a lesser degree. The cross-correlations of the final features are shown in Figure S1.

Beyond removing correlated features, we further aim to improve interpretability by retaining only a subset of the remaining features that best predict PWS. Specifically, we retained only three features each from the climate, soil, and topography categories, so that the importances of the different categories can be more easily compared without the complicating role of there being different numbers of features in different categories. The final features chosen and their data sources are also detailed in Table 1.

TABLE 1 Input features for the random forest model.

Category	Name	Source	Data reference
Soil	Bulk density, 0–50 cm	gNATSGO	Soil Survey Staff (2023)
	Saturated hydraulic conductivity, 0–50 cm ( $K_{s, \max}$ )	gNATSGO	Soil Survey Staff (2023)
	Root-zone water storage (RZ storage)	See ref.	McCormick et al. (2021)
Topography	Slope	NED	Gesch et al. (2002)
	Aspect	NED	Gesch et al. (2002)
	Topographic wetness index (TWI)	MERIT HYDRO	Yamazaki et al. (2019)
Vegetation	Mean NDVI	MODIS MOD13Q1	Didan (2021)
Climate	Mean VPD	PRISM	Daly et al. (2015)
	Coefficient of variation of precipitation	PRISM	Daly et al. (2008)
	Aridity index	gridMET	Abatzoglou (2013)



### 3 | RESULTS

As shown in Figure 1a, the selected FIA sites span the forests (and in some cases, shrublands) of the western United States. Although the criteria for establishing dominance of a single species exclude more sites in some locations than others, most regions with forest cover measured by FIA have at least some sites included in our dataset. The regions where focusing on dominant-species sites excludes the most forest land include northern California, central Oregon, western Idaho, and eastern Nevada. Considering only locations where a single species dominates the basal area inevitably biases the species distribution somewhat, as some species may be more likely to grow in areas with little species diversity (e.g., plantations). Still, the five most common species by basal area in the western United States are represented in the analyzed sites, including Douglas-fir (*Pseudotsuga menziesii*, 3553 sites), ponderosa pine (*Pinus ponderosa*, 2373 sites), Utah juniper (*Juniperus osteosperma*, 2063 sites), and lodgepole pine (*Pinus contorta*, 1121 sites). One exception is the western hemlock (*Tsuga heterophylla*), for which only 145 sites are included in our final dataset. Several genera are likely under-represented in our dataset relative to western forests as a whole, but nevertheless include a reasonably large sample size. These include several oak (e.g., Gambel oak, *Quercus gambelii*, 473 sites and blue oak, *Quercus douglasii*, 174 sites), fir (e.g., white fir, *Abies concolor*, 273 sites, and subalpine fir, *Abies lasiocarpa*, 286 sites), and spruce (e.g., Engelmann spruce, *Picea engelmannii*, 381 sites) species. Other common species in our dataset include honey mesquite (*Prosopis glandulosa*, 2692 sites) and oneseed juniper (*Juniperus monosperma*, 1142 sites). The number of sites for the top five most common sites is compared graphically in Figure 1b.

The PWS varies considerably within species. Although the exact shape of the distribution of PWS (Figure 2, showing the top 5 most common species in the region) varies from species to species, all distributions are relatively wide and overlap considerably. Indeed,

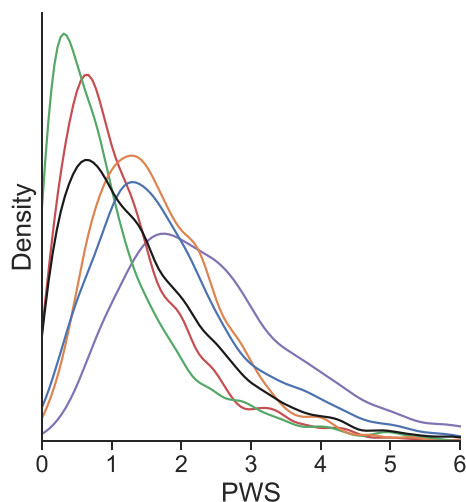


**FIGURE 2** PWS probability density for the top five most common species among the dataset used (colored lines) and for all sites (black line), plotted using kernel density estimation.

when considering all species that have at least 50 dominant pixels (to ensure sufficient sample size), and calculating the species mean of each, the standard deviation of the species-mean PWS values is 0.27. By contrast, the average standard deviation of PWS across sites with the same dominant species is 0.91. That is, the mean values of PWS for each species are much less variable than the PWS is across different sites with the same dominant species. This suggests that species knowledge can provide information about PWS, but not fully constrain it. Indeed, using the species-specific mean PWS value to predict PWS variation explains only 23% of observed variability in PWS (Figure 3a). By contrast, using a random forest driven by geographic factors allows for 43% of observed variability to be explained—almost double (Figure 3b). This number was relatively consistent across the 10 cross-validation folds of the random forest model, varying between 40% and 46%.

The errors in the random forest predictions are largest for low values of PWS, and values of PWS below 0.6 are never predicted, despite making up 25% of observations. Similarly, the species-average model predicts a value of PWS < 0.6 in only 3% of conditions. If low PWS values cannot be explained by either species models or the random forest model, this may point to the influence of LFMC retrieval errors in these pixels, since these would tend to reduce the calculated PWS values. High PWS values (e.g., greater than 3) are rarely predicted by the species-based model, but are a common random forest prediction that matches observations in areas such as Eastern Arizona and Southern Texas (Figure S2).

The random forest predictions are particularly sensitive to mean VPD and mean NDVI, which are almost or more than twice as important as the other features (Figure 4a). Mean NDVI is cross-correlated with mean precipitation ( $r = .74$ ) across the study sites. Mean VPD is also partially cross-correlated (e.g. absolute cross-correlations between 0.4 and 0.6) with several other features (aridity index, bulk density, slope, TWI; Figure S1), likely because of its strong dependence on temperature, and thus elevation. Based on accumulated local effects plots of the four most important features (Figure 5), mean NDVI and mean VPD are particularly important at low NDVI and high VPD values, respectively. Thus, the combined effect of climate aridity and vegetation density is most important in the drier regions of the western United States, that is, outside of higher elevation, densely forested areas. When all other features are held constant, the PWS first decreases with mean NDVI until it reaches a value of approximately 0.35, and then increases slowly with NDVI. The initial decline in sensitivity with NDVI may be because areas with greater NDVI (and thus more canopy) are also expected to have deeper and more laterally extensive roots (Mao et al., 2018; Tumber-Dávila et al., 2022), allowing for greater access to water reserves that allow sustained water uptake even during drier periods. By contrast, at NDVI values greater than 0.35, the expected greater loss of water to transpiration because of greater leaf area may lead the PWS to stop decreasing and instead increase slightly. The accumulated local effect of mean VPD on PWS increases continuously with VPD (particularly in the driest regions with the greatest VPD, as discussed above), consistent with previous findings by D'Orangeville

**FIGURE 3** Variability in PWS predicted by (a) the observed species-mean PWS for the dominant species at each site and (b) the random forest of climate, plant trait, soil, and topographic factors. Narrow-bandwidth kernel density estimation was applied for visualization purposes; lighter colors indicate greater density. For each panel, the one-to-one line is shown in blue.

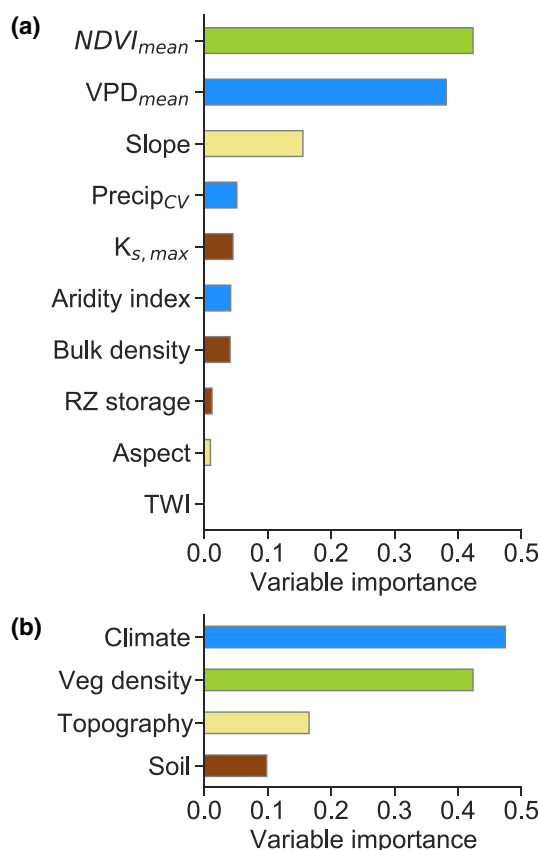
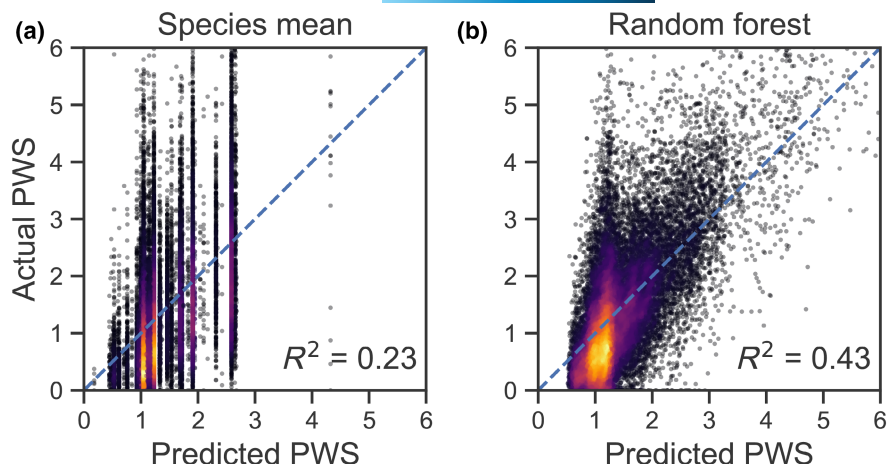


**FIGURE 4** Variable importance of input features for the region-wide random forest model predicting PWS, individually (Panel a) and aggregated by feature type (Panel b). In panel a, individual input features are colored by their category type. Panel (b) shows the relative importance of climatic descriptions (blue), vegetation density (green), topographic descriptors (yellow), and soil properties (brown) in the random forest model. For each category except vegetation density, the relative importance shown is the sum of that calculated for all three features in each category. Because each category contains the same number of features, the sum of the individual feature importances can be compared more easily. The exception is the vegetation density, for which only a single feature was used to avoid confounding influences from the high cross-correlations between vegetation density metrics.

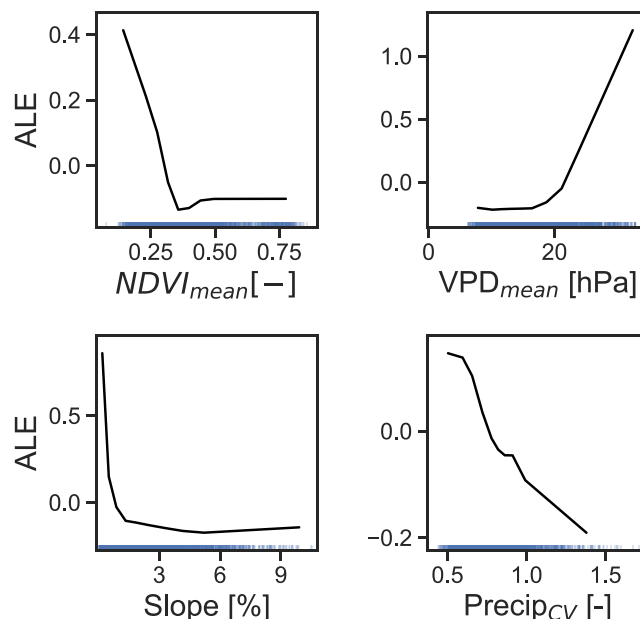


**FIGURE 5** Accumulated local effects plots for the four most important random forest features. The tick marks along each axis represent the relative density of the distribution of that variable across all sites studied.

et al. (2018) that growth responses to drought are stronger in areas with greater long-term mean potential evapotranspiration. The accumulated local effects plots also show that, counter-intuitively, PWS decreases with increasing slope, particularly for low slopes less than 1%. A possible explanation for this pattern is that these extremely flat areas receive little lateral flow run-off from other areas, and thus, all else held constant, depend more strongly on local climate (and have greater PWS as a result). For sufficiently high values (e.g., in sufficiently steep terrain), this reverses, with the significantly greater precipitation losses to run-off in higher slope areas increasing plant water sensitivity. Lastly, the accumulated local effect of the coefficient of variation of precipitation on PWS with the coefficient of variation of precipitation is positive. That is, if all other features are held constant, areas with more variable rain have lower PWS.

This may be initially surprising, as more variable rainfall may be expected to effectively decrease water availability to forests (because water is more likely to run off, or because more variable rainfall may be associated with longer dry seasons). Thus, the response of PWS to the coefficient of variation of rainfall may be expected to have the same sign as the response to mean VPD, while Figure 4 shows the opposite is the case. This complexity reflects the multi-faceted nature of plant responses to water stress, with trait adaptations to minimize vulnerability leading to a range of transpiration (and thus, possible LFMC) responses, and vice versa (Feng et al., 2017).

Overall, the random forest model is likely to include some compensating errors because not all possible covariates of PWS are included in the model, and because some cross-correlations remain between the input features of the model (and between input features and other variables that are not included in the model but may plausibly affect PWS, see Table S1). We therefore do not interpret the accumulated local effects plot of features that are less important to the random forest predictions, and focus on the explained variability of the model predictions rather than the model itself.

Further insight can be gained by aggregating the feature importance by type (Figure 4b). Note that in Figure 4b, the only vegetation density feature contributing to the importance is the mean NDVI, whereas the climate, topography, and soil categories represent the sum of the importance of each category's three features. Climate features are the most important category, but despite only being able to capture one dimension of 'vegetation density' through mean NDVI, the vegetation density category is nevertheless the second-most important, and is more than twice as important as the topography category and more than four times as important as the soil category. By contrast, the topographic category (including slope, aspect, and topographic wetness index) and the soils category (including the saturated soil hydraulic conductivity, maximum root-zone water storage, and bulk density) has only a relatively small importance for the region-wide model. This may be because topographic and soil features are only relevant in a smaller subset of temporal (e.g., particularly wet) or spatial (e.g., particularly steep) conditions. The explained variability of random forest models built with only one feature type at a time (e.g., only climate, only soil, etc.) (Figure S3) is also consistent with the patterns in Figure 4b.

## 4 | DISCUSSION

### 4.1 | Species type only partially influences plant water stress sensitivity

Only 23% of the spatial variability in PWS is explained by which species is dominant. This relatively low number may be partially explained by noise in our PWS dataset, including the simplifying assumption of linearity in the PWS calculation (Equation 1) and the presence of noise in the LFMC and DFMC sets. Additionally, we calculate a single PWS for each pixel based on the response of LFMC to meteorological aridity over a 6-year period. Six years is not enough to fully average over

climatic variability, and thus the degree of water stress on the vegetation varies across space not just because of difference in vegetation behavior between pixels, but also because of the different distribution/amount of meteorological aridity observed during the study period (Slette et al., 2019). While the climate during the 6 years used to calculate PWS is close to that across a much longer 42-year period across pixels (Figure S4), the relatively short 6-year period may still be a source of error at individual pixels. Nevertheless, the 43% of spatial variability in PWS explained by the random forest model puts a bound on the degree to which noise limits the explanatory power of the PWS patterns. It provides context for the 23% explanatory power of species information, which is considerably lower than 43%. That is, only 53% (0.23/0.43) of total explainable PWS variations can be explained by species information alone. This suggests that, while a considerable amount of PWS is dependent on the dominant species, other factors (such as changes in soil, topography, vegetation density, or adaptation to mean climate) are almost as important as which species is dominant for predicting local plant sensitivity to water stress.

Note that although several of the factors considered in the random forest model are cross-correlated with species dominance (because species tend to grow in specific climate and biogeographical niches), this does not affect our conclusion of significant controls of other factors. The geographic distribution of species may affect the finding that 43% of PWS spatial variability can be explained, but not that species-explained variability is only 53% of total explainable variability. That is, because the random forest explains almost twice as much of the spatial variability in PWS as a mathematically optimal species-only model does, factors beyond cross-correlations between species niches and the random forests' input features must be contributing substantially to the total 43% observed variability of the random forest model.

Our result is consistent with a previous finding that growth sensitivity to drought in Eastern North American forests are often more variable within species than between them (D'Orangeville et al., 2018). Such consistency is not surprising, as many of the factors causing environmentally driven differences in PWS also affect growth rates, and many of the processes controlling growth responses to drought are likely to also influence plant water stress response across a range of hydrometeorological conditions.

Several other factors may contribute to the low explanatory variability of species, including but not limited to the features considered in the random forest model. For example, the amount of water available to vegetation at any point depends on a number of factors. These include the degree to which rainfall ends up as root-available water under different conditions—as influenced by, for example, the seasonal timing of rainfall (Romme et al., 2009) or by topographic factors that affect what fraction of rainfall runs off either above- or belowground and how quickly, for example, Fan et al. (2019). Other factors include soil texture and its effect on both water retention and the amount of water that can be stored in the soil (Hahm et al., 2019). These factors are partially captured in the features that we consider. However, other properties such as variability in soil properties with depth (De Kauwe et al., 2015), sub-grid scale hillslope distribution and



orientation (Fan et al., 2019), and groundwater or rock moisture interactions (Giardina et al., 2023; McCormick et al., 2021; Miguez-Macho & Fan, 2021) likely also play a role. Furthermore, transpiration from understory species (which are not captured here) also responds to—and feeds back on—soil water availability (McIver et al., 2022). Locations with greater average root-available water likely also support greater stand density or leaf area, which in turn influences rates of water loss and thus, PWS (Bottero et al., 2017). Lastly, while hydraulic traits vary substantially between species, they can also exhibit non-negligible intra-specific variability. For example, Rosas et al. (2019) examined sources of variability across several plant hydraulic traits in six tree species, and found that for a majority of traits studied, intra-specific variability accounted for roughly 20%–45% of total variability in that trait. Additionally, across a hydrologic gradient in the Amazon, intra-specific variability in P50 for two species was 76% and 97% of the local community's inter-specific variation, respectively (with equivalent ratios of 55% and 63% for wood density) (Garcia et al., 2022).

We note that the 23% explanatory power of species information we calculated may also be limited by the strong assumption that the dominant species in FIA plots are also dominant over the entire 4 km PWS pixel (as long as the PWS pixel's dominant land cover class is consistent with the dominant species type of the FIA plot). This assumption is likely violated in at least some of the 21,455 pixels studied. Nevertheless, the value of studying species effects across a domain as large as the entire western United States is expected to outweigh the disadvantages of this strong simplifying assumption. Thus, the conclusion that other factors are at least as important as which species is dominant in controlling local sensitivity to hydroclimate is likely to be robust.

Overall, our results imply that studies of inter-specific differences in plant water stress response should also explicitly consider the environments in which observations for each species are made, and whether those environments are representative of the entire species range. If the study sites lie at the extreme end of the species' climatic range or, to a lesser degree, in unusual soil and topographic conditions, the conclusions of the study may not be robust everywhere in the range. Such analyses of study site 'representativeness' are currently quite rare. Yet they can be performed for many species, facilitated by efforts to aggregate species occurrence records like the Global Biodiversity Information Facility (GBIF, Robertson et al., 2014). Additionally, our findings point to the utility of considering not just a single study site when analyzing a particular species, but studying the same species' behavior across an expansive network of study sites (e.g., Cabon et al., 2023; Lockwood et al., 2023; Novick, Jo, et al., 2022), so that the roles of climate, soil, and topography are at least partially integrated.

## 4.2 | Relative importance of controls beyond species on PWS variability

The random forest cross-validation  $R^2$  is on par with the explained variability in several other studies of different plant water stress

response metrics (e.g.,  $R^2 = .36$  for trees in Ukkola et al. (2021),  $R^2 = .38$ –.46 for Fu et al. (2022),  $R^2 = .39$  and .52 for Yang et al. (2022)), building confidence in its implied relative importance of different factors. Nevertheless, the fact that many known controls on PWS are not included because their variation across the western United States is poorly mapped (e.g., groundwater and rock moisture influences on root water uptake, stand age and disturbance history, etc.) likely limits the explained variability of the random forest model.

Mean NDVI, a partial proxy for vegetation density, is intimately tied to plant water use, explaining its role as the most important feature of the random forest model. Greater NDVI suggests greater leaf area, and thus, all else being equal, greater water loss rates through transpiration. Indeed, it has long-been hypothesized that canopy density in a given environment acts to minimize the average water stress (Eagleson, 1982). At the tree scale, growth sensitivity to drought has been shown to vary with rates of intra-species competition (which is expected to be greater at greater stand density), and with stand density itself (e.g., Bottero et al., 2017; Gleason et al., 2017). As a result, either externally imposed or self-incurred thinning processes can reduce plant growth sensitivity to drought (Giuggiola et al., 2013; Jump et al., 2017; Thomas & Waring, 2015). The high importance of mean NDVI in the random forest model suggests that such density-dependence is highly important even when water uptake and loss patterns are considered (as is the case here), rather than the previously studied growth responses to drought.

Climatic factors also have high importance in the random forest model, consistent with previous studies of drought sensitivity (D'Orangeville et al., 2018; Felton et al., 2021; Fu et al., 2022; Ukkola et al., 2021). Indeed, D'Orangeville et al. (2018) and Fu et al. (2022) also found a particularly large role for evaporative demand and VPD, respectively, in studies of growth response to drought and sensitivity of evaporative fraction to soil moisture. This is consistent with mean VPD being the second-most important feature in our study.

Several factors likely explain why climatic factors are so important for explaining the PWS spatial variability (Figure 4b). Mean climate is a first order control on water availability at a site, and thus on the likelihood of hydrologic stress. Additionally, several individual studies have shown the potential for significant plant trait adaptation to climate (Blackman et al., 2017; Depardieu et al., 2020; Pritzkow et al., 2020; Tuomela, 1997). Finally, there are likely some methodological artifacts. For example, although the specific vegetation density and climatic factors used as input features in the random forest model have been chosen to minimize cross-correlation, they are far from zero (Figure S1). Likewise, mean NDVI is highly cross-correlated with several climate features. For example,  $r_{\text{mean NDVI, mean annual precipitation}} = .74$ . Thus, the exact explanatory power of vegetation density versus climatic factors may be difficult to disentangle. Further, the mean DFMC and temporal standard deviation of DFMC have a low to intermediate cross-correlation with climate variables used in the random forest model ( $r = -.34$  to .25, Figure S5). This is roughly on par with the cross-correlation between PWS and aridity index ( $r = -.20$ ) and only slightly lower than the cross-correlation between PWS and

mean VPD ( $r = .38$ ). Even in the absence of a causative relationship between the climate features and PWS, the cross-correlation between mean climate and the DFMC patterns used to calculate PWS may therefore create an artificial dependence of PWS on climate. It is, however, difficult to imagine how one might design a metric of plant sensitivity to water limitations that is not sensitive to such cross-correlations. Overall, we expect the high importance of climate features for the random forest to reflect a combination of artificial cross-correlations and substantial true influences of climate on PWS. This suggests efforts to improve the parametrization of plant traits related to water stress in land surface models (Anderegg, 2015; Liu et al., 2021) might benefit from incorporating relationships between traits and climate (Famiglietti et al., 2023; Wu et al., 2020).

The relatively low influence of soil properties in the model (Figure 4b) is surprising, particularly in light of the expected high quality of the gNATSGO data used to derive soil properties. This may be because the role of soil properties is quite temporally variable (e.g., saturated hydraulic conductivity is likely to be quite important in very wet conditions, whereas wilting point or retention parameters would be more important influences on root-zone water availability during dry conditions). In addition, the most relevant depths of the soil properties likely also vary across space and time (whereas we assume a constant averaging depth of 50 cm). Finally, the low influence of soil properties could also be influenced by soil-vegetation interactions that are not accounted for here, such as rock moisture uptake (Fan et al., 2019; McCormick et al., 2021), root effects on soil structure (Fatichi et al., 2020), or soil-hydraulic parameter relationships that are not accounted for more generally (e.g., pedo-transfer function uncertainty (Novick, Ficklin, et al., 2022; Paschalis et al., 2022)). Despite the relatively low influence of soil properties on PWS found here, more research is needed to assess how soil hydraulics influence large-scale patterns of ecosystem sensitivity to water stress.

## 5 | CONCLUSIONS

In this study, we analyzed the relative influence of species and other factors across tens of thousands of forested locations across the Western United States. By coupling a remotely sensed measure of PWS with species dominance information from FIA plots, we are able to analyze the drivers of regional scale behavior without ignoring the role of species variability or without relying on species-specific means obtained from trait databases (e.g., Anderegg et al., 2018; Trugman et al., 2020). Species explain a significant, but not a dominant, amount of the variability in PWS. This suggests that efforts to account for species distributions in land surface models (Quetin et al., 2023) may improve representation of ecosystem responses to water stress. However, it also implies that species-specific studies of water stress responses may provide only limited information if the locations they study are not representative of the typical environment in which that species grows. Thus, species-specific studies

should study individuals of a species across a range of the climate, soil, and topographic environments in which it grows. Our result that many different factors contribute to the overall ecosystem-scale sensitivity of vegetation to hydroclimatic variability is with a number of previous studies (e.g., D'Orangeville et al., 2018; Green et al., 2022; Ukkola et al., 2021). However, the large influence of site-specific climate factors shown here suggests that further research is needed to quantify the amount of plasticity of plant hydraulic traits to climate across a wide range of species and biogeographic conditions.

## AUTHOR CONTRIBUTIONS

**Alexandra G. Konings:** Conceptualization; data curation; funding acquisition; investigation; methodology; software; visualization; writing – original draft; writing – review and editing. **Krishna Rao:** Conceptualization; data curation; investigation; methodology; software; writing – review and editing. **Erica L. McCormick:** Data curation; methodology; software; writing – review and editing. **Anna T. Trugman:** Data curation; methodology; writing – review and editing. **A. Park Williams:** Conceptualization; methodology; writing – review and editing. **Noah S. Diffenbaugh:** Conceptualization; methodology; writing – review and editing. **Marta Yebra:** Conceptualization; methodology; writing – review and editing. **Meng Zhao:** Data curation; methodology; software; writing – review and editing.

## ACKNOWLEDGEMENTS

AGK was funded by NSF DEB grant 1942133, by NASA grant 80NSSC21K1523 from the Modeling Analysis and Prediction program, and by the Alfred P. Sloan Foundation. AGK, ATT, and APW acknowledge funding from the Gordon and Betty Moore Foundation under grant # 11974. This paper is a contribution of the Western Fire and Forest Resilience Collaborative. ELM was funded by the NSF Graduate Research Fellowship. NSD acknowledges support from Stanford University. ATT also acknowledges funding from NSF Grants 2003205 and 2216855.

## CONFLICT OF INTEREST STATEMENT

The authors declare no conflicts of interest.

## DATA AVAILABILITY STATEMENT

The LFMC data used to calculate PWS are available at <https://doi.org/10.5281/zenodo.12618505>. FIA data are available at <https://www.fia.fs.usda.gov/tools-data/>. All other input features are from publicly available datasets described in Table 1. The data structures containing the assembled PWS, species cover, and other input features at each of FIA sites studied here are available from Dryad at doi: [10.5061/dryad.g1jwstr05](https://doi.org/10.5061/dryad.g1jwstr05). The analysis code used in this manuscript is available from doi: [10.5281/zenodo.12676807](https://doi.org/10.5281/zenodo.12676807) and GitHub at <https://github.com/agkonings/PWSSpeciesAnalysis>.

## ORCID

Alexandra G. Konings  <https://orcid.org/0000-0002-2810-1722>

Krishna Rao  <https://orcid.org/0000-0002-8912-0441>

Erica L. McCormick  <https://orcid.org/0000-0002-7160-398X>  
 Anna T. Trugman  <https://orcid.org/0000-0002-7903-9711>  
 A. Park Williams  <https://orcid.org/0000-0001-8176-8166>  
 Noah S. Diffenbaugh  <https://orcid.org/0000-0002-8856-4964>  
 Marta Yebra  <https://orcid.org/0000-0002-4049-9315>  
 Meng Zhao  <https://orcid.org/0000-0001-6883-865X>

## REFERENCES

- Abatzoglou, J. T. (2013). Development of gridded surface meteorological data for ecological applications and modelling. *International Journal of Climatology*, 33(1), 121–131. <https://doi.org/10.1002/joc.3413>
- Anderegg, W. R. L. (2015). Spatial and temporal variation in plant hydraulic traits and their relevance for climate change impacts on vegetation. *New Phytologist*, 205(3), 1008–1014. <https://doi.org/10.1111/nph.12907>
- Anderegg, W. R. L., Trugman, A. T., Badgley, G., Anderson, C. M., Bartuska, A., Ciais, P., Cullenward, D., Field, C. B., Freeman, J., Goetz, S. J., Hicke, J. A., Huntzinger, D., Jackson, R. B., Nickerson, J., Pacala, S., & Randerson, J. T. (2020). Climate-driven risks to the climate mitigation potential of forests. *Science*, 368(6497), eaaz7005. <https://doi.org/10.1126/science.aaz7005>
- Anderegg, W. R., Konings, A. G., Trugman, A. T., Yu, K., Bowling, D. R., Gabbitas, R., Karp, D. S., Pacala, S., Sperry, J. S., Sulman, B. N., & Zenes, N. (2018). Hydraulic diversity of forests regulates ecosystem resilience during drought. *Nature*, 561(7724), 538–541.
- Bartlett, M. K., Klein, T., Jansen, S., Choat, B., & Sack, L. (2016). The correlations and sequence of plant stomatal, hydraulic, and wilting responses to drought. *Proceedings of the National Academy of Sciences of the United States of America*, 113(46), 13098–13103. <https://doi.org/10.1073/pnas.1604088113>
- Bechtold, W. A., & Patterson, P. L. (2005). *The enhanced forest inventory and analysis program—national sampling design and estimation procedures*. No. 80. USDA Forest Service, Southern Research Station.
- Beven, K. J., & Kirkby, M. J. (1979). A physically based, variable contributing area model of basin hydrology / un modèle à base physique de zone d'appel variable de l'hydrologie du bassin versant. *Hydrological Sciences Bulletin*, 24(1), 43–69. <https://doi.org/10.1080/02626667909491834>
- Blackman, C. J., Aspinwall, M. J., Tissue, D. T., & Rymer, P. D. (2017). Genetic adaptation and phenotypic plasticity contribute to greater leaf hydraulic tolerance in response to drought in warmer climates. *Tree Physiology*, 37(5), 583–592. <https://doi.org/10.1093/treephys/tpx005>
- Bottero, A., D'Amato, A. W., Palik, B. J., Bradford, J. B., Fraver, S., Battaglia, M. A., & Asherin, L. A. (2017). Density-dependent vulnerability of forest ecosystems to drought. *Journal of Applied Ecology*, 54(6), 1605–1614. <https://doi.org/10.1111/1365-2664.12847>
- Brodribb, T. J., Powers, J., Cochard, H., & Choat, B. (2020). Hanging by a thread? Forests and drought. *Science*, 368(6488), 261–266. <https://doi.org/10.1126/science.aat7631>
- Brzostek, E. R., Dragoni, D., Schmid, H. P., Rahman, A. F., Sims, D., Wayson, C. A., Johnson, D. J., & Phillips, R. P. (2014). Chronic water stress reduces tree growth and the carbon sink of deciduous hardwood forests. *Global Change Biology*, 20(8), 2531–2539. <https://doi.org/10.1111/gcb.12528>
- Buckley, T. N. (2017). Modeling stomatal conductance. *Plant Physiology*, 174(2), 572–582. <https://doi.org/10.1104/pp.16.01772>
- Burgan, R. (1988). *Revisions to the 1978 National Fire Danger Rating System*. (USDA Forest Service, Southeastern Forest Experimental Station Research Paper No. SE-273). Asheville, NC.
- Burrill Elizabeth, A., DiTommaso Andrea, M., Turner Jeffery, A., Pugh Scott, A., Menlove James, C. G., Perry Carol, J., & Conkling Barbara, L. (2021). The forest inventory and analysis database: Database description and user guide for phase 2 (Version 9.0. 1). Database Documentation. Last modified September, 29, 2023.
- Cabon, A., DeRose, R. J., Shaw, J. D., & Anderegg, W. R. L. (2023). Declining tree growth resilience mediates subsequent forest mortality in the US Mountain West. *Global Change Biology*, 29(17), 4826–4841. <https://doi.org/10.1111/gcb.16826>
- Coffield, S. R., Hemes, K. S., Koven, C. D., Goulden, M. L., & Randerson, J. T. (2021). Climate-driven limits to future carbon storage in California's wildland ecosystems. *AGU Advances*, 2(3), e2021AV000384. <https://doi.org/10.1029/2021AV000384>
- Cohen, J. D., & Deeming, J. E. (1985). *The national fire-danger rating system: Basic equations*. Pacific Southwest Forest and Range Experiment Station, Forest Service, U.S. Department of Agriculture; Gen. Tech. Rep. PSW-82. 16 p, 082. <https://doi.org/10.2737/PSW-GTR-82>
- D'Orangeville, L., Maxwell, J., Kneeshaw, D., Pederson, N., Duchesne, L., Logan, T., Houle, D., Arseneault, D., Beier, C. M., Bishop, D. A., Druckenbrod, D., Fraver, S., Girard, F., Halman, J., Hansen, C., Hart, J. L., Hartmann, H., Kaye, M., Leblanc, D., ... Phillips, R. P. (2018). Drought timing and local climate determine the sensitivity of eastern temperate forests to drought. *Global Change Biology*, 24(6), 2339–2351. <https://doi.org/10.1111/gcb.14096>
- Daly, C., Halbleib, M., Smith, J. I., Gibson, W. P., Doggett, M. K., Taylor, G. H., Curtis, J., & Pasteris, P. P. (2008). Physiographically sensitive mapping of climatological temperature and precipitation across the conterminous United States. *International Journal of Climatology*, 28(15), 2031–2064. <https://doi.org/10.1002/joc.1688>
- Daly, C., Smith, J. I., & Olson, K. V. (2015). Mapping atmospheric moisture Climatologies across the conterminous United States. *PLoS One*, 10(10), e0141140. <https://doi.org/10.1371/journal.pone.0141140>
- De Kauwe, M. G., Zhou, S.-X., Medlyn, B. E., Pitman, A. J., Wang, Y.-P., Duursma, R. A., & Prentice, I. C. (2015). Do land surface models need to include differential plant species responses to drought? Examining model predictions across a mesic-xeric gradient in Europe. *Biogeosciences*, 12(24), 7503–7518. <https://doi.org/10.5194/bg-12-7503-2015>
- Depardieu, C., Girardin, M. P., Nadeau, S., Lenz, P., Bousquet, J., & Isabel, N. (2020). Adaptive genetic variation to drought in a widely distributed conifer suggests a potential for increasing forest resilience in a drying climate. *New Phytologist*, 227(2), 427–439. <https://doi.org/10.1111/nph.16551>
- Didan, K. (2021). MODIS/Terra vegetation indices 16-Day L3 global 250m SIN Grid V061 [Data set]. NASA EOSDIS land processes distributed active archive center. <https://doi.org/10.5067/MODIS/MOD13Q1.061>
- Eagleson, P. S. (1982). Ecological optimality in water-limited natural soil-vegetation systems: 1. Theory and hypothesis. *Water Resources Research*, 18(2), 325–340. <https://doi.org/10.1029/WR018i002p00325>
- Famiglietti, C. A., Worden, M., Quetin, G. R., Smallman, T. L., Dayal, U., Bloom, A. A., Williams, M., & Konings, A. G. (2023). Global net biome CO<sub>2</sub> exchange predicted comparably well using parameter–environment relationships and plant functional types. *Global Change Biology*, 29(8), 2256–2273.
- Fan, Y., Clark, M., Lawrence, D. M., Swenson, S., Band, L. E., Brantley, S. L., Brooks, P. D., Dietrich, W. E., Flores, A., Grant, G., Kirchner, J. W., Mackay, D. S., McDonnell, J. J., Milly, P. C. D., Sullivan, P. L., Tague, C., Ajami, H., Chaney, N., Hartmann, A., ... Yamazaki, D. (2019). Hillslope hydrology in global change research and earth system modeling. *Water Resources Research*, 55(2), 1737–1772. <https://doi.org/10.1029/2018WR023903>
- Fatichi, S., Or, D., Walko, R., Vereecken, H., Young, M. H., Ghezzehei, T. A., Hengl, T., Kollet, S., Agam, N., & Avissar, R. (2020). Soil structure is an important omission in earth system models. *Nature Communications*, 11(1), 522. <https://doi.org/10.1038/s41467-020-14411-z>

- Faticchi, S., Pappas, C., & Ivanov, V. Y. (2016). Modeling plant–water interactions: An ecohydrological overview from the cell to the global scale. *WIREs Water*, 3(3), 327–368. <https://doi.org/10.1002/wat2.1125>
- Felton, A. J., Shriver, R. K., Bradford, J. B., Suding, K. N., Allred, B. W., & Adler, P. B. (2021). Biotic vs abiotic controls on temporal sensitivity of primary production to precipitation across north American drylands. *New Phytologist*, 231(6), 2150–2161. <https://doi.org/10.1111/nph.17543>
- Feng, X., Dawson, T. E., Ackerly, D. D., Santiago, L. S., & Thompson, S. E. (2017). Reconciling seasonal hydraulic risk and plant water use through probabilistic soil–plant dynamics. *Global Change Biology*, 23(9), 3758–3769. <https://doi.org/10.1111/gcb.13640>
- Fry, J. A., Xian, G., Jin, S., Dewitz, J. A., Homer, C. G., Yang, L., Barnes, C., Herold, N., & Wickham, J. (2011). Completion of the 2006 national land cover database for the conterminous United States. *Photogrammetric Engineering & Remote Sensing*, 77(9), 858–864.
- Fu, Z., Ciais, P., Feldman, A. F., Gentine, P., Makowski, D., Prentice, I. C., Stoy, P. C., Bastos, A., & Wigneron, J. P. (2022). Critical soil moisture thresholds of plant water stress in terrestrial ecosystems. *Science Advances*, 8(44), eabq7827. <https://doi.org/10.1126/sciadv.abq7827>
- Garcia, M. N., Hu, J., Domingues, T. F., Groenendijk, P., Oliveira, R. S., & Costa, F. R. C. (2022). Local hydrological gradients structure high intraspecific variability in plant hydraulic traits in two dominant central Amazonian tree species. *Journal of Experimental Botany*, 73(3), 939–952. <https://doi.org/10.1093/jxb/erab432>
- Gazol, A., Camarero, J. J., Anderegg, W. R. L., & Vicente-Serrano, S. M. (2017). Impacts of droughts on the growth resilience of northern hemisphere forests. *Global Ecology and Biogeography*, 26(2), 166–176. <https://doi.org/10.1111/geb.12526>
- Gesch, D., Oimoen, M., Greenlee, S., Nelson, C., Steuck, M., & Tyler, D. (2002). The national elevation dataset. *Photogrammetric Engineering and Remote Sensing*, 68(1), 5–32.
- Giardina, F., Gentine, P., Konings, A. G., Seneviratne, S. I., & Stocker, B. D. (2023). Diagnosing evapotranspiration responses to water deficit across biomes using deep learning. *New Phytologist*, 240(3), 968–983. <https://doi.org/10.1111/nph.19197>
- Giuggiola, A., Bugmann, H., Zingg, A., Dobbertin, M., & Rigling, A. (2013). Reduction of stand density increases drought resistance in xeric scots pine forests. *Forest Ecology and Management*, 310, 827–835. <https://doi.org/10.1016/j.foreco.2013.09.030>
- Gleason, K. E., Bradford, J. B., Bottero, A., D'Amato, A. W., Fraver, S., Palik, B. J., Battaglia, M. A., Iverson, L., Kenefic, L., & Kern, C. C. (2017). Competition amplifies drought stress in forests across broad climatic and compositional gradients. *Ecosphere*, 8(7), e01849. <https://doi.org/10.1002/ecs2.1849>
- González de Andrés, E., Rosas, T., Camarero, J. J., & Martínez-Vilalta, J. (2021). The intraspecific variation of functional traits modulates drought resilience of European beech and pubescent oak. *Journal of Ecology*, 109(10), 3652–3669. <https://doi.org/10.1111/1365-2745.13743>
- Gray, A., Brandeis, T., Shaw, J., McWilliams, W., & Miles, P. (2012). Forest inventory and analysis database of The United States of America (FIA). *Biodiversity & Ecology*, 4, 225–231. <https://doi.org/10.7809/b-e.00079>
- Green, J. K., Ballantyne, A., Abramoff, R., Gentine, P., Makowski, D., & Ciais, P. (2022). Surface temperatures reveal the patterns of vegetation water stress and their environmental drivers across the tropical Americas. *Global Change Biology*, 28(7724), 2940–2955. <https://doi.org/10.1111/gcb.16139>
- Grossiord, C., Buckley, T. N., Cernusak, L. A., Novick, K. A., Poulter, B., Siegwolf, R. T. W., Sperry, J. S., & McDowell, N. G. (2020). Plant responses to rising vapor pressure deficit. *New Phytologist*, 226(6), 1550–1566. <https://doi.org/10.1111/nph.16485>
- Hahn, W. J., Dralle, D. N., Rempe, D. M., Bryk, A. B., Thompson, S. E., Dawson, T. E., & Dietrich, W. E. (2019). Low subsurface water storage capacity relative to annual rainfall decouples Mediterranean plant productivity and water use from rainfall variability. *Geophysical Research Letters*, 46(12), 6544–6553. <https://doi.org/10.1029/2019GL083294>
- Jump, A. S., Ruiz-Benito, P., Greenwood, S., Allen, C. D., Kitzberger, T., Fensham, R., Martínez-Vilalta, J., & Lloret, F. (2017). Structural overshoot of tree growth with climate variability and the global spectrum of drought-induced forest dieback. *Global Change Biology*, 23(9), 3742–3757. <https://doi.org/10.1111/gcb.13636>
- Kannenberg, S. A., Guo, J. S., Novick, K. A., Anderegg, W. R. L., Feng, X., Kennedy, D., Konings, A. G., Martínez-Vilalta, J., & Matheny, A. M. (2022). Opportunities, challenges and pitfalls in characterizing plant water-use strategies. *Functional Ecology*, 36(1), 24–37. <https://doi.org/10.1111/1365-2435.13945>
- Knighton, J., & Berghuijs, W. R. (2023). Water ages explain tradeoffs between long-term evapotranspiration and ecosystem drought resilience. *Geophysical Research Letters*, 50(10), e2023GL103649. <https://doi.org/10.1029/2023GL103649>
- Liu, L., Zhang, Y., Wu, S., Li, S., & Qin, D. (2018). Water memory effects and their impacts on global vegetation productivity and resilience. *Scientific Reports*, 8(1), 2962. <https://doi.org/10.1038/s41598-018-21339-4>
- Liu, Y., Kumar, M., Katul, G. G., Feng, X., & Konings, A. G. (2020). Plant hydraulics accentuates the effect of atmospheric moisture stress on transpiration. *Nature Climate Change*, 10(7), 691–695. <https://doi.org/10.1038/s41558-020-0781-5>
- Liu, Y., Holtzman, N. M., & Konings, A. G. (2021). Global ecosystem-scale plant hydraulic traits retrieved using model–data fusion. *Hydrology and Earth System Sciences*, 25(5), 2399–2417. <https://doi.org/10.5194/hess-25-2399-2021>
- Lockwood, B. R., Maxwell, J. T., Denham, S. O., Robeson, S. M., LeBlanc, D. C., Pederson, N., Novick, K. A., & Au, T. F. (2023). Interspecific differences in drought and pluvial responses for *Quercus alba* and *Quercus rubra* across the eastern United States. *Agricultural and Forest Meteorology*, 340, 109597. <https://doi.org/10.1016/j.agrfo.2023.109597>
- Lu, Y., Sloan, B., Thompson, S. E., Konings, A. G., Bohrer, G., Matheny, A., & Feng, X. (2022). Intra-specific variability in plant hydraulic parameters inferred from model inversion of sap flux data. *Journal of Geophysical Research: Biogeosciences*, 127(6), e2021JG006777. <https://doi.org/10.1029/2021JG006777>
- Mao, W., Felton, A. J., Ma, Y., Zhang, T., Sun, Z., Zhao, X., & Smith, M. D. (2018). Relationships between aboveground and belowground trait responses of a dominant plant species to alterations in water-table depth. *Land Degradation & Development*, 29(11), 4015–4024. <https://doi.org/10.1002/ldr.3159>
- Mastrotheodoros, T., Pappas, C., Molnar, P., Burlando, P., Manoli, G., Parajka, J., Rigon, R., Szeles, B., Bottazzi, M., Hadjidoukas, P., & Faticchi, S. (2020). More green and less blue water in the Alps during warmer summers. *Nature Climate Change*, 10(2), 155–161. <https://doi.org/10.1038/s41558-019-0676-5>
- Matthews, S. (2014). Dead fuel moisture research: 1991–2012. *International Journal of Wildland Fire*, 23(1), 78. <https://doi.org/10.1071/WF13005>
- McColl, K. A., Alemohammad, S. H., Akbar, R., Konings, A. G., Yueh, S., & Entekhabi, D. (2017). The global distribution and dynamics of surface soil moisture. *Nature Geoscience*, 10(2), 100–104. <https://doi.org/10.1038/ngeo2868>
- McCormick, E. L., Dralle, D. N., Hahn, W. J., Tune, A. K., Schmidt, L. M., Chadwick, K. D., & Rempe, D. M. (2021). Widespread woody plant use of water stored in bedrock. *Nature*, 597(7875), 225–229. <https://doi.org/10.1038/s41586-021-03761-3>
- McIver, J., Grace, J. B., & Roundy, B. (2022). Piñon and juniper tree removal increases available soil water, driving understory response in a sage-steppe ecosystem. *Ecosphere*, 13(11), e4279. <https://doi.org/10.1002/ecs2.4279>



- Miguez-Macho, G., & Fan, Y. (2021). Spatiotemporal origin of soil water taken up by vegetation. *Nature*, 598(7882), 624–628. <https://doi.org/10.1038/s41586-021-03958-6>
- Miralles, D. G., Gentile, P., Seneviratne, S. I., & Teuling, A. J. (2019). Land-atmospheric feedbacks during droughts and heatwaves: State of the science and current challenges. *Annals of the New York Academy of Sciences*, 1436(1), 19–35. <https://doi.org/10.1111/nyas.13912>
- Novick, K. A., Ficklin, D. L., Baldocchi, D., Davis, K. J., Ghezzehei, T. A., Konings, A. G., MacBean, N., Raoult, N., Scott, R. L., Shi, Y., Sulman, B. N., & Wood, J. D. (2022). Confronting the water potential information gap. *Nature Geoscience*, 15(3), 158–164. <https://doi.org/10.1038/s41561-022-00909-2>
- Novick, K. A., Jo, I., D'Orangeville, L., Benson, M., Au, T. F., Barnes, M., Denham, S., Fei, S., Heilman, K., Hwang, T., Keyser, T., Maxwell, J., Miniati, C., McLachlan, J., Pederson, N., Wang, L., Wood, J., & Phillips, R. (2022). The drought response of eastern US oaks in the context of their declining abundance. *Bioscience*, 72(4), 333–346. <https://doi.org/10.1093/biosci/biab135>
- Novick, K. A., Ficklin, D. L., Stoy, P. C., Williams, C. A., Bohrer, G., Oishi, A. C., Papuga, S. A., Blanken, P. D., Noormets, A., Sulman, B. N., Scott, R. L., Wang, L., & Phillips, R. P. (2016). The increasing importance of atmospheric demand for ecosystem water and carbon fluxes. *Nature Climate Change*, 6(11), 1023–1027. <https://doi.org/10.1038/nclimate3114>
- Pappas, C., Faticchi, S., & Burlando, P. (2016). Modeling terrestrial carbon and water dynamics across climatic gradients: Does plant trait diversity matter? *New Phytologist*, 209(1), 137–151. <https://doi.org/10.1111/nph.13590>
- Paschalis, A., Bonetti, S., Guo, Y., & Faticchi, S. (2022). On the uncertainty induced by Pedotransfer functions in terrestrial biosphere modeling. *Water Resources Research*, 58(9), e2021WR031871. <https://doi.org/10.1029/2021WR031871>
- Pritzkow, C., Williamson, V., Szota, C., Trouvé, R., & Arndt, S. K. (2020). Phenotypic plasticity and genetic adaptation of functional traits influences intra-specific variation in hydraulic efficiency and safety. *Tree Physiology*, 40(2), 215–229. <https://doi.org/10.1093/treephys/tpz121>
- Quetin, G. R., Anderegg, L. D. L., Boving, I., Anderegg, W. R. L., & Trugman, A. T. (2023). Observed forest trait velocities have not kept pace with hydraulic stress from climate change. *Global Change Biology*, 29, 5415–5428. <https://doi.org/10.1111/gcb.16847>
- Rao, K., Williams, A. P., Diffenbaugh, N. S., Yebra, M., & Konings, A. G. (2022). Plant-water sensitivity regulates wildfire vulnerability. *Nature Ecology & Evolution*, 6(3), 332–339. <https://doi.org/10.1038/s41559-021-01654-2>
- Rao, K., Williams, A. P., Flefil, J. F., & Konings, A. G. (2020). SAR-enhanced mapping of live fuel moisture content. *Remote Sensing of Environment*, 245, 111797. <https://doi.org/10.1016/j.rse.2020.111797>
- Robertson, T., Döring, M., Guralnick, R., Bloom, D., Wiczorek, J., Braak, K., Otegui, J., Russell, L., & Desmet, P. (2014). The GBIF integrated publishing toolkit: Facilitating the efficient publishing of biodiversity data on the internet. *PLoS One*, 9(8), e102623. <https://doi.org/10.1371/journal.pone.0102623>
- Romme, W. H., Allen, C. D., Bailey, J. D., Baker, W. L., Bestelmeyer, B. T., Brown, P. M., Eisenhart, K. S., Floyd, M. L., Huffman, D. W., Jacobs, B. F., Miller, R. F., Muldavin, E. H., Swetnam, T. W., Tausch, R. J., & Weisberg, P. J. (2009). Historical and modern disturbance regimes, stand structures, and landscape dynamics in Piñon-Juniper vegetation of the Western United States. *Rangeland Ecology & Management*, 62(3), 203–222. <https://doi.org/10.2111/08-188R1.1>
- Rosas, T., Mencuccini, M., Barba, J., Cochard, H., Saura-Mas, S., & Martínez-Vilalta, J. (2019). Adjustments and coordination of hydraulic, leaf and stem traits along a water availability gradient. *New Phytologist*, 223(2), 632–646. <https://doi.org/10.1111/nph.15684>
- Rossiter, D. G., Poggio, L., Beaudette, D., & Libohova, Z. (2022). How well does digital soil mapping represent soil geography? An investigation from the USA. *The Soil*, 8(2), 559–586. <https://doi.org/10.5194/soil-8-559-2022>
- Sabot, M. E. B., De Kauwe, M. G., Pitman, A. J., Medlyn, B. E., Ellsworth, D. S., Martin-StPaul, N. K., Wu, J., Choat, B., Limousin, J.-M., Mitchell, P., Rogers, A., & Serbin, S. (2022). One stomatal model to rule them all? Toward improved representation of carbon and water exchange in global models. *Journal of Advances in Modeling Earth Systems*, 14(4), e2021MS002761. <https://doi.org/10.1029/2021MS002761>
- Seager, R., Ting, M., Li, C., Naik, N., Cook, B., Nakamura, J., & Liu, H. (2013). Projections of declining surface-water availability for the southwestern United States. *Nature Climate Change*, 3(5), 482–486. <https://doi.org/10.1038/nclimate1787>
- Serra-Maluquer, X., Gazol, A., Anderegg, W. R. L., Martínez-Vilalta, J., Mencuccini, M., & Camarero, J. J. (2022). Wood density and hydraulic traits influence species' growth response to drought across biomes. *Global Change Biology*, 28(12), 3871–3882. <https://doi.org/10.1111/gcb.16123>
- Simard, M., Pinto, N., Fisher, J. B., & Baccini, A. (2011). Mapping forest canopy height globally with spaceborne lidar. *Journal of Geophysical Research: Biogeosciences*, 116(G4), 4021. <https://doi.org/10.1029/2011JG001708>
- Skelton, R. P., West, A. G., & Dawson, T. E. (2015). Predicting plant vulnerability to drought in biodiverse regions using functional traits. *Proceedings of the National Academy of Sciences of the United States of America*, 112(18), 5744–5749. <https://doi.org/10.1073/pnas.1503376112>
- Slette, I. J., Post, A. K., Awad, M., Even, T., Punzalan, A., Williams, S., Smith, M. D., & Knapp, A. K. (2019). How ecologists define drought, and why we should do better. *Global Change Biology*, 25(10), 3193–3200. <https://doi.org/10.1111/gcb.14747>
- Soil Survey Staff. (2023). Gridded national soil survey geographic (gNATSGO) database for the conterminous United States. United States Department of Agriculture, Natural Resources Conservation Service. <https://nrcs.app.box.com/v/soils>
- Thomas, Z., & Waring, K. M. (2015). Enhancing resiliency and restoring ecological attributes in second-growth ponderosa pine stands in northern New Mexico, USA. *Forest Science*, 61(1), 93–104. <https://doi.org/10.5849/forsci.13-085>
- Trugman, A. T., Anderegg, L. D. L., Shaw, J. D., & Anderegg, W. R. L. (2020). Trait velocities reveal that mortality has driven widespread coordinated shifts in forest hydraulic trait composition. *Proceedings of the National Academy of Sciences of the United States of America*, 117(15), 8532–8538.
- Tumber-Dávila, S. J., Schenk, H. J., Du, E., & Jackson, R. B. (2022). Plant sizes and shapes above and belowground and their interactions with climate. *New Phytologist*, 235(3), 1032–1056. <https://doi.org/10.1111/nph.18031>
- Tuomela, K. (1997). Leaf water relations in six provenances of *Eucalyptus microtheca*: A greenhouse experiment. *Forest Ecology and Management*, 92(1), 1–10. [https://doi.org/10.1016/S0378-1127\(96\)03961-8](https://doi.org/10.1016/S0378-1127(96)03961-8)
- Ukkola, A. M., De Kauwe, M. G., Pitman, A. J., Best, M. J., Abramowitz, G., Haverd, V., Decker, M., & Houghton, N. (2016). Land surface models systematically overestimate the intensity, duration and magnitude of seasonal-scale evaporative droughts. *Environmental Research Letters*, 11(10), 104012. <https://doi.org/10.1088/1748-9326/11/10/104012>
- Ukkola, A. M., De Kauwe, M. G., Roderick, M. L., Burrell, A., Lehmann, P., & Pitman, A. J. (2021). Annual precipitation explains variability in dryland vegetation greenness globally but not locally. *Global Change Biology*, 27(18), 4367–4380. <https://doi.org/10.1111/gcb.15729>
- Ukkola, A. M., Prentice, I. C., Keenan, T. F., van Dijk, A. I. J. M., Viney, N. R., Myneni, R. B., & Bi, J. (2016). Reduced streamflow in water-stressed climates consistent with CO<sub>2</sub> effects on vegetation. *Nature Climate Change*, 6(1), 75–78. <https://doi.org/10.1038/nclimate2831>



- Vargas Zeppetello, L. R., McColl, K. A., Bernau, J. A., Bowen, B. B., Tang, L. I., Holbrook, N. M., Gentine, P., & Huybers, P. (2023). Apparent surface conductance sensitivity to vapour pressure deficit in the absence of plants. *Nature Water*, 1(11), 941–951. <https://doi.org/10.1038/s44221-023-00147-9>
- Wang, Y., Köhler, P., He, L., Doughty, R., Braghiere, R. K., Wood, J. D., & Frankenberg, C. (2021). Testing stomatal models at the stand level in deciduous angiosperm and evergreen gymnosperm forests using CLIMA land (v0.1). *Geoscientific Model Development*, 14(11), 6741–6763. <https://doi.org/10.5194/gmd-14-6741-2021>
- Wu, C., Coffield, S. R., Goulden, M. L., Randerson, J. T., Trugman, A. T., & Anderegg, W. R. L. (2023). Uncertainty in US forest carbon storage potential due to climate risks. *Nature Geoscience*, 16(5), 422–429. <https://doi.org/10.1038/s41561-023-01166-7>
- Wu, G., Hu, Z., Keenan, T. F., Li, S., Zhao, W., Cao, R. C., Li, Y., Guo, Q., & Sun, X. (2020). Incorporating spatial variations in parameters for improvements of an evapotranspiration model. *Journal of Geophysical Research: Biogeosciences*, 125(11), e2019JG005504. <https://doi.org/10.1029/2019JG005504>
- Xu, L., Saatchi, S. S., Yang, Y., Yu, Y., Pongratz, J., Bloom, A. A., Bowman, K., Worden, J., Liu, J., Yin, Y., Domke, G., McRoberts, R. E., Woodall, C., Nabuurs, G. J., de-Miguel, S., Keller, M., Harris, N., Maxwell, S., & Schimel, D. (2021). Changes in global terrestrial live biomass over the 21st century. *Science Advances*, 7(27), eabe9829.
- Yamazaki, D., Ikeshima, D., Sosa, J., Bates, P. D., Allen, G. H., & Pavelsky, T. M. (2019). MERIT Hydro: A high-resolution global hydrography map based on latest topography dataset. *Water Resources Research*, 55(6), 5053–5073. <https://doi.org/10.1029/2019WR024873>
- Yang, H., Ciais, P., Wigneron, J.-P., Chave, J., Cartus, O., Chen, X., Fan, L., Green, J. K., Huang, Y., Joetzjer, E., Kay, H., Makowski, D., Maignan, F., Santoro, M., Tao, S., Liu, L., & Yao, Y. (2022). Climatic and biotic factors influencing regional declines and recovery of tropical forest biomass from the 2015/16 El Niño. *Proceedings of the National Academy of Sciences of the United States of America*, 119(26), e2101388119. <https://doi.org/10.1073/pnas.2101388119>
- Zhao, M., Aa, G., Liu, Y., & Konings, A. (2022). Evapotranspiration frequently increases during droughts. *Nature Climate Change*, 12(11), 1024–1030. <https://doi.org/10.1038/s41558-022-01505-3>

## SUPPORTING INFORMATION

Additional supporting information can be found online in the Supporting Information section at the end of this article.

**How to cite this article:** Konings, A. G., Rao, K., McCormick, E. L., Trugman, A. T., Williams, A. P., Diffenbaugh, N. S., Yebra, M., & Zhao, M. (2024). Tree species explain only half of explained spatial variability in plant water sensitivity. *Global Change Biology*, 30, e17425. <https://doi.org/10.1111/gcb.17425>